IJL, Issue 2, Vol. 23, 2024
https://doi.org/10.31900/ijl.v23i2.485

Research Article

IRAQI JOURNAL OF LASER

Photonic crystal fiber drug sensor based on surface plasmon resonance

Sally K. Abbas* and Soudad S. Ahmed

Department of physics, college of science, university of Baghdad, Baghdad, Iraq
** Email address of the Corresponding Author:sallyaljanabi@gmail.com*

Article history: Received 30 Jun. 2024; Revised 14 Aug. 2024; Accepted 3 Sept. 2024; Published online15 Dec. 2024

Abstract: This study introduces a sensor using Photonic Crystal Fiber (PCF) and Surface Plasmon Resonance (SPR) technology. Gold (Au) was applied as a thin coating on a PCF, which had been previously coated with a chemically stable gold compound that exhibits plasmonic properties. The thickness of the gold coating was 40nm. The performance metrics, such as sensitivity (including wavelength sensitivity and amplitude sensitivity) and resolution, were assessed by simulation via the COMSOL program. The suggested sensor was developed utilizing the finite element method and then subjected to numerical analysis. The findings indicate that the surface of Photonic Crystal Fiber when coated with Au, functions as a sensor for detecting the refractive index (IR) of expired pharmaceutical samples. Research is conducted on the effects of the structural parameters on the resonant spectra with the aim of enhancing sensing performance. The highest amplitude sensitivity recorded was 31.2 RIU-1, whereas the maximum resolution reached was 6×10-5 RIU. These measurements were obtained within the detection range of 1.383 to 1.399.

Keywords: COMSOL, PCF, pharmaceutical samples, surface plasmon resonance.

1. Introduction

Many fields rely on optical fiber sensors, including academia, environmental monitoring, and the field of communication technology. Reasons for this include their size, sensitivity, electrical passivity, immunity to electromagnetic interference, bandwidth, and suitability for use in tip-based sensing applications. The majority of these optical sensors detect changes in the refractive index (RI) of a gas or liquid by measuring differences in optical characteristics [1]. The reflectance index (RI) is a crucial metric for characterizing the optical characteristics of fluids. Biotechnology methods [2] also provide important information on drug/DNA interaction and cell growth [3], and this has led to the advancement of RI sensors for use in numerous sectors, including water salinity assessment [4]. Photonic Crystal Fiber (PCF) sensors utilize the propagation of surface plasmons. Due to their high sensitivity, ease of integration, rapid reaction, and immediate findings, they are extensively employed for refractive index monitoring.

When p-polarized light and surface plasmons (SP) reach a phase-matching condition, they stimulate a charge density oscillation at the interface between a metal and a dielectric element, this optical phenomenon

is known as surface plasmon resonance (SPR) [5-9]. PCF-SPR sensors, which integrate the benefits of PCF technology and plasmonic science, have been devised to monitor environmental conditions [10], ascertain solution concentration [11], facilitate water quality control, aid in biomedical treatment [12], identify gases, assist in health diagnostics, and further [13].The evanescent field is the key of PCF-SPR's sensing mechanism. When light of a particular wavelength penetrates the PCF's fiber core and partly passes through its cladding, a transient field is generated. Surface plasmon waves arise from the interaction between electrons in a plasmonic metal surface (such as copper, gold, silver, or aluminum) with evanescent fields. Once the core guiding mode's refractive index (RI) approaches that of the SPPi modes, phase matchings take place, and the two modes are now linked. [14, 15].

PCF-SPR technology addresses the limitations of traditional prism-based SPR sensing, such as large size, the need for precise incidence angle, and many mechanical parts. These limitations restrict distant sensing capabilities and limit the range of applications [16]. Based on sensor assessment, two different sensing modalities are distinguished: interior and outside. The analyte is cast off to charge up the air hole or a metal coating is put around the core in internal sensing or sensing based on nanowires. Positioning plasmonic material outside to act as a sensing medium for exterior applications including D-shape, slit, and microchannel sensors is an additional way to use plasmonic material [17].

A D-shaped PCF sensor based on SPR that was covered by a 40 nm gold layer was suggested by Jassam et al. [18]. Its highest resolution was 4 x 10-5 RIU, and it had an amplitude sensitivity of 99.2 RIU-1 within the detection range of 1.351-1.363. A PCF~SPRr sensor was developed by Mahmood et al. and demonstrated an impressive sensitivity of 164.3 nm/RIU throughout the 1.33–1.3431 analyte refractive index range. The coating that the researchers applied to the air holes was made of plasmonic material, namely gold. They then used analyte samples to fill up these gaps [19]. This effort, however, used an internal sensing approach to substantially improve the sensor's performance. Therefore, by effectively integrating the core-guiding mode with the SPP mode, the performance of the sensor was improved. Due to their small fiber diameter, complicated structure, and tiny air hole diameter, most of the PCF conformations that have been studied were challenging to produce. While the majority of PCF-SPR sensors have undergone mathematical analysis, ESM-12-02 has been subjected to analysis in conjunction with the finite element technique (FEM) for SPR. The manufactured PCF has six air holes organized in a regular pattern around a tiny core. When it comes to sensor resolution and amplitude sensitivity, the suggested framework could provide the greatest sensitivity available.

2. Theoretical investigation and design of sensors

A. Sellmeier Equation

The suggested sensor mostly utilizes silica in its fabrication. All of the openings in the structure are devoid of any substance and are instead occupied by air. The refractive index of silica is defined by equation 1 [20].

$$N_{silica} = 1 + \frac{a_1 \lambda^2}{\lambda^2 - b_1} + \frac{a_2 \lambda^2}{\lambda^2 - b_2} + \frac{a_3 \lambda^2}{\lambda^2 - b_3} \quad (1)$$

Silica's refractive index, denoted as N, is dependent on the wavelength, λ, which is measured in μm. The Sellmeier constants for silica are represented by the sets (a1, a2, a3) and (b1, b2, b3) correspondingly. a1=0.6961663, a2=0.4079426, a3= 0.8974794.

B. Drude–Lorentz Model

At higher frequencies, the real and imaginary components of the dielectric constant cannot be estimated using the Drude model. By expressing the interband effect (IB) as the sum of Lorentzian functions, it may be avoided.

A simple representation of the frequency-dependent dielectric function is $\varepsilon(\omega)=\varepsilon Drude(\omega)+\varepsilon IB(\omega)$. Equation 2 may be used to express the dispersion relation of gold, a noble metal, using the Drude-Lorentz model [21].

$$\varepsilon_{Au} = \varepsilon_{\alpha} - \frac{\omega_D^2}{\omega(\omega+j\gamma_{D)}} - \frac{\Delta\varepsilon.\Omega_L^2}{(\omega^2-\Omega_L^2)+j\Gamma_L\omega} \quad (2)$$

In this case, εAu stands for the gold substance's permittivity, whereas ε∞ is the gold's permittivity at a high frequency, which is 5.9673. You may express the angular frequency, ω, as ω = 2πc / λ, where c is the speed of light in a vacuum. At 2113.6 THz, the plasma frequency is ωD/2π, while at 15.92 THz, the damping frequency is γD/2π. At 1.09, the weighting factor Δε is set. The Lorentz oscillators have an oscillator power of 650.07 THz and a spectral width of 104.86 THz. While Ω_L and Γ_L are the oscillator strength and spectral width of the Lorentz oscillators

3. Photonic Crystal Fiber designed for Endlessly Single Model

The Single-Mode Solid Core PCF, especially the ESM~12~02 type provided by Thorlabs Assembly, has a stable mode field diameter and shows negligible loss across a wide range of wavelengths from 200 nm to over 2000 nm. An industry standard, the ESM-12-02 has an outside length of 125 µm and is well-matched with most fiber equipment. When it came to sensors, interferometers, and applications that needed short wavelengths like visible light and ultraviolet (UV) radiation, the ESM-12-02 was the way to go. It could produce wideband radiation in a single spatial mode. The physicochemical features of ESM-12-02 are listed in Table 1.

Table 1. Physical properties of PCF.

Photonic crystal fiber Properties	
Core diameter	10.2µm
Holes diameter	2.46µm
Pitch	7.8µm
Outside diameter	125µm

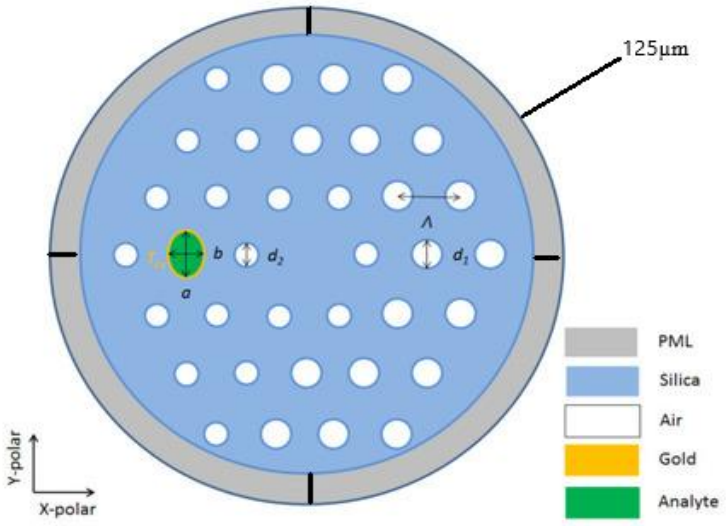

Fig. 1: Cross-sectional observation of the suggested sensor.

The NKT Photonics ESM-12 PCF is specifically engineered to function as a single-mode fiber, maintaining a constant outside length of 125 µm. It works with any fiber tool that is widely used. Figure 1 displays a graphic representation of the PCF~SPR sensor created by the use of the COMSOL MULTPHYSICS tool. After the PCF received a 40 nm covering of plasmonic matter, such as gold, the sample was deposited onto it. As the boundary media, a Perfectly Matched Layer (PML) was used to effectively absorb the scattered light that was directed toward the surface of the fiber. The PML is a round sheet with a thickness of 12 µm in the proposed construction. The convergence experiments were effectively conducted and subsequently adjusted to produce more precise results by adjusting the PML width and mesh sizing.

4. Results and Discussion

When a specified wavelength is produced by the phase of the Surface Plasmon Polariton mode and core controlling in a certain material, resonance results. The connection between the basic mode for y-polarisations and the dispersion of the Second Surface Plasmon Polariton (SSPP) mode is shown in Figure 2. Another thing that this picture shows with the red line is the structure's general propagation mode's confinement loss. An evident decrease in intensity at the specific wavelength of 658 nm was observed, indicating the alignment of the core with the 2nd surface plasmon polariton mode. Consequently, the SPP mode acquires the most amount of energy from the fundamental core mode. In the y-polarization, Figure 2 shows the distribution of the electric field for the phase-matching core mode (b) and the fundamental core-guiding mode (a).

The results were obtained with the analyte having a refractive index of 1.383 and a phase-matching condition used. Even small changes in the analyte's refractive index might have a significant impact on the loss of depth. The suggested PCF sensor's loss spectrum is shown in Figure 3 for different n_a values. Redshift occurred as the peak shifted towards longer wavelengths as the depth of loss increased. This is so because the phase matching point varies with increasing effectual refractive index of the surface plasmon mode. This results in a decreased difference between the core-guided mode and the plasmon mode, hence improving the efficiency of coupling. The maximum attenuation coefficient of 5.79 dB/cm was observed at a wavelength of 658 nm, corresponding to a refractive index of 1.383. The power transmission between the core and SPP phases was more intense as the loss depth increased. The result was caused by an elevation in the refractive index of the substance being analyzed. Therefore, the resonant spectrum was further limited.

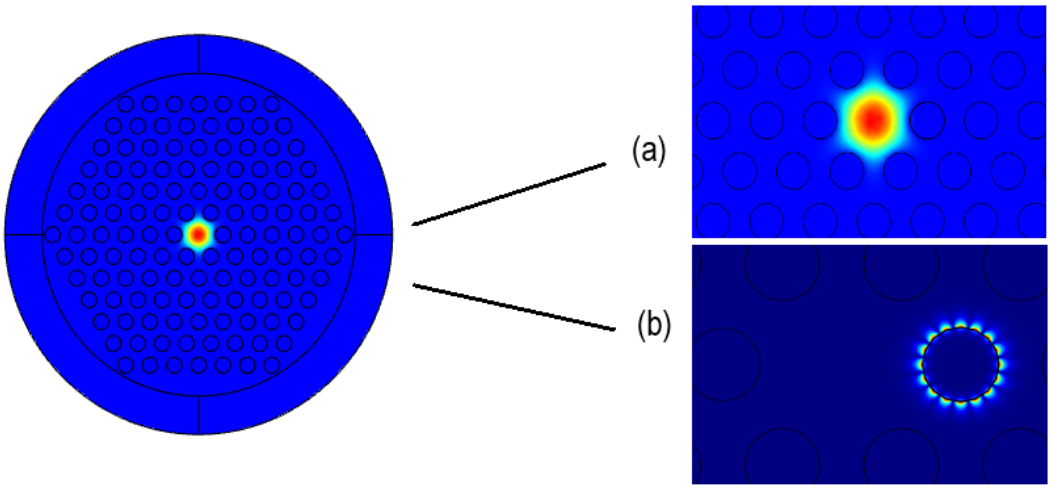

Fig. 2: Electric field distributions at na =1.383 in (a) core-guided mode, (b) SPP mode (y-polarized).

When the refractive index of the analyte increases as shown in Figure 4 the peak loss reduces. This is due to a poorer coupling efficiency caused by a larger variance between the plasmon mode and core guided and a decreased n_{eff} of the plasmon mode that varies the phase corresponding point.

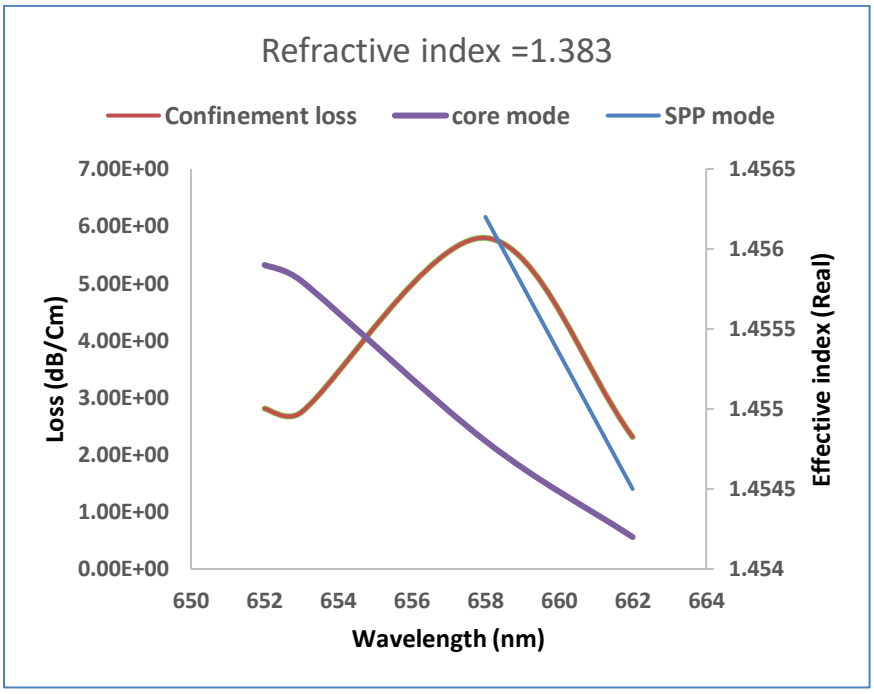

Fig. 3: Dispersion relation between core guiding mode and the second Surface plasmon mode.

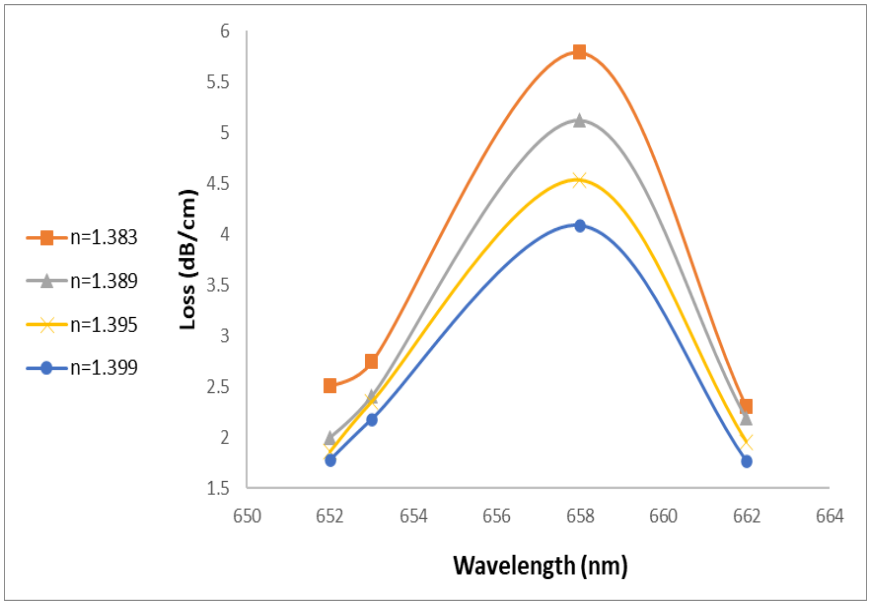

Fig. 4: The confinement loss spectrum of the proposed Photonic Crystal Fiber (PCF) Surface Plasmon Resonance (SPR) sensor varies as the analyte's refractive index (RI) increases from 1.383 to 1.399.

Amplification consideration and wavelength approaches may be employed to evaluate the operation of the planned sensor. Equation (3) is applicable for the calculation of wavelength sensitivity [22]:

$$S_W(\lambda) = \frac{\Delta\lambda_{peak}}{\Delta n_a} \quad (3)$$

The resonant peaks and the fluctuation in the analyte's refractive index are represented by the values of Δλ peak and Δna, respectively.

The proposed sensor is sensitive to wavelengths of 1667 nm/RIU for na = 1.383, 1.389, and 1.395. The resonant wavelength peaks occur at 10 nm for variations in the refractive index of the analyte within the ranges of 1.383-1.389, 1.389-1.395, and 1.395-1.399. These ranges indicate the intervals amongst the points of resonant wavelength. The sensor's resolution is a crucial feature that characterizes its ability to spot even the slightest alteration in the refractive index of the analyte. The resolution (R) of the suggested sensor was denoted by Eq. 4 [22]:

$$R = \frac{\Delta na \times \Delta\lambda min}{\Delta\lambda peak}\ [RIU] \quad (4)$$

The variables in the issue are as follows: The slightest spectral resolution is denoted by $\Delta\lambda_{min}$, while the greatest shift in the resonant wavelength peak is represented by $\Delta\lambda_{peak}$. The change in refractive index (RI) of the analyte or sample is represented by n_a. The greatest resolution achieved was 6×10^{-5} RIU, based on the assumptions that Δn_a (change in refractive index) is 0.006, $\Delta\lambda_{min}$ (minimum change in wavelength) is 0.1, n_a (refractive index) is 1.399, and $\Delta\lambda_{peak}$ (change in peak wavelength) is 10 nm. Finding the sensor's amplitude sensitivity is possible with the help of Equation (5) [22]:

$$S_A(\lambda) = -\frac{1}{\alpha(\lambda,n_a)}\frac{\partial\alpha(\lambda,n_a)}{\partial n_a}[RIU^{-1}] \quad (5)$$

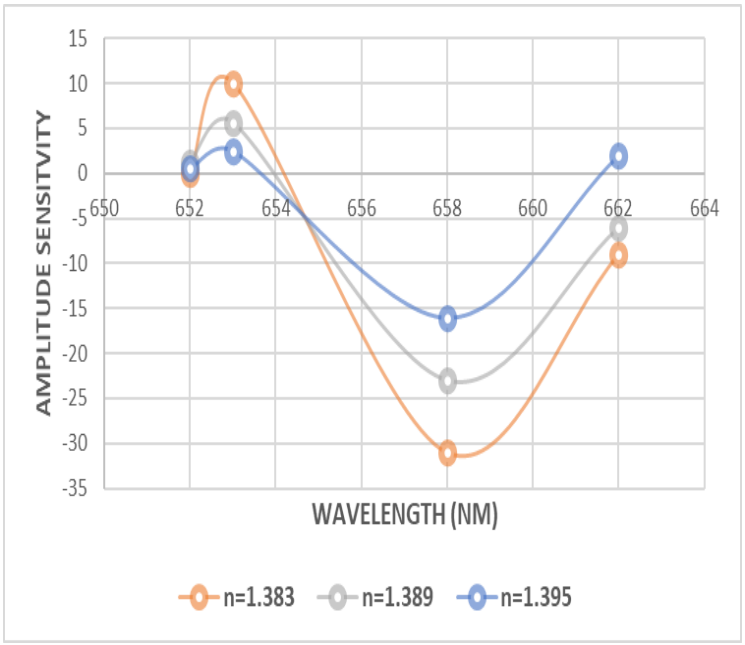

Fig. 5: The amplitude sensitivity changes as the wavelength varies, while the refractive index of the sample increases from 1.383 to 1.399.

In contrast to ∂α (λ, na), which represents the change in confinement loss among two analyte samples with identical refractive indices, α (λ, na) represents the analyte's confinement loss at a certain refractive index. The level of reactivity of different analyte/sample refractive indices is shown in Figure 5. The maximum amplitude sensitivity values were 16 RIU^{-1}, 23.34 RIU^{-1}, and 31.2 RIU^{-1} for refractive index variations of the analyte/sample within the ranges of 1.383-1.389, 1.389-1.395, and 1.395-1.399, respectively.

5. Conclusion

This study utilizes a Photonic Crystal Fiber sensor that operates on the principle of surface Plasmon Resonance (PCF-SPR) to identify expired medication samples. The sensor is designed by applying a gold layer to the air hole located on the right side of the PCF core. Analyzing the resonant wavelength or confinement loss spectrum peak with the actual component of the effective index of the core guiding mode and surface plasmon mode may help identify the unknown material. The Finite Element Method (FEM) was used to examine the basic mode sensor characteristics. The maximum wavelength at which the sensor is sensitive is 1667 nm/RIU, and the maximum amplitude at which it is sensitive is 31.2 RIU^{-1}. These sensitivities were observed within the detecting range of 1.383 to 1.399. The suggested sensor has the potential to function as a biosensor, thanks to its simple design and exceptional sensing capabilities.

References

[1] S.K. Abbas, S.S. Ahmed, "Refractive index sensor based on tapered photonic crystal fiber to determine the performance of different carbonated liquids", J Opt (2023).
[2] D. Pereira, O. Frazão, and J. Santos, "Fiber Bragg grating sensing system for simultaneous measurement of salinity and temperature", Optical Engineering, 43, 299–304 (2004).
[3] F. Jiménez-Márquez, J. Vázquez, J. Úbeda, and J. Sánchez-Rojas, "Low- cost and portable refractive opteoelectronic device for measuring wine fermentation kinetics", Sensors and Actuators B Chemical, 178, 316–323 (2013).
[4] S. Silva, P. Roriz, and O. Frazão, "Refractive index measurement of liquids based on microstructured optical fibers", Photonics, 1, 516-529 (2014).
[5] G. M. Jassam, S. S Ahmed, "Acetic acid concentration estimation using plastic optical fiber sensor-based surface plasmon resonance", Iraqi J. Phys. 17, 11 (2019).
[6] N. S. Rahim, S. S. Ahmed, and M. F. Sultan, "Optical fiber biomedical sensor based on surface plasmon resonance", Iraqi J. Sci. 61, 1650-1656 (2020).
[7] E. Khatar and S. S. Bassam, "Surface Plasmon Plastic Optical Fiber Resonance with Multi-Layer as Chemical Sensor", Iraqi J. Phys. 19, 51 (2021).
[8] N. S. Rahim, S. S. Bassam, "Estimating sugar concentration in human blood serum using Surface Plasmon Resonance (SPR) –based optical fiber sensor", Iraqi J. Phys. 17, 41 (2019).
[9] G. M. Jassam, S. S. Alâ, and M. F. Sultan, "Fabrication of a chemical sensor based on surface plasmon resonance via plastic optical fiber", Iraqi J. Sci. 61, 765 (2020).
[10] N. F. Muhammed, A. I. Mahmood, Sh. A. Kadhim, and I. A. Naseef, "Simulation Design of Hollow Core Photonic Crystal fiber for Sensing Water Quality", J Phys: Conf Ser. 1530 012134 (2020).
[11] S. Maheswaran, P. Kuppusamy, S. Ramesh, T. Sundararajan, and P. Yupapin, "Refractive index sensor using dual core photonic crystal fiber–glucose detection applications", Results Phys., 11, 577– 578 (2018).
[12] M. AF. Gatea, A. H. Jawad, "Thermoplasmonic of single Au@SiO_2 and SiO_2@Au core shell nanoparticles in deionized water and polyvinylpyrrolidone matrix", Baghdad Sci J., 916(2), 0376 (2019).
[13] H. Yuan, W. Ji, S. Chu, Q. Liu, S. Qian, J. Guang, et al. "Mercaptopyridine functionalized gold nanoparticles for fiber-optic surface plasmon resonance Hg2+ sensing", ACS Sens., 4(3), 704–710 (2019)
[14] A. K. Paul, "Graphene-Coated Highly Sensitive Photonic Crystal Fiber Surface Plasmon Resonance Sensor for Aqueous Solution: Design and Numerical Analysis", OSA Contin. 3, 2253 (2020).
[15] M. Li, J. Xu, Q. Zheng, C. Guo, and Y. Chen, "Chemical-based surface plasmon resonance imaging of fingerprints", Analyt. Chem. 94, 7238 (2022).
[16] M. T. Rahman, S. Datto, and M. N. Sakib, "Highly sensitive circular slotted gold-coatedmicro channel photonic crystal fiber basedplasmonic biosensor", OSA Contin. 4, 1808 (2021).

[17] A. A. Rifat, M. R. Hasan, R. Ahmed, and H. Butt, "Spiral Photonic Crystal Fiber Based Dual- Polarized Surface Plasmon Resonance Biosensor", J. Nanophot. 12, 012503 (2018).
[18] G.M. Jassam, S.S. Ahmed, "Tapered PCF Mach–Zehnder interferometer based on surface plasmon resonance (SPR) for estimating concentration toxic metal ions (lead)", J Opt 53, 163–168 (2024).
[19] A. I. Mahmood, R. K. Ibrahim, A. I. Mahmood, and Z. K. Ibrahim, "Design and simulation of surface plasmon resonance sensors for environmental monitoring", J. Phys.: Conf. Ser. (IOP Publishing), p. 012118, (2018).
[20] S. Islam, J. Sultana, A. A. Rifat, R. Ahmed, A. Dinovitser, B. W. H. Ng, H. Ebendorff-Heidepriem, and D. Abbott, "Dual-Polarized Highly Sensitive Plasmonic Sensor in the Visible to Near-IR Spectrum," Opt. Express, vol. 26, no. 23, pp. 30347–30361 (2018).
[21] A. Vial, A. S. Grimault, D. Macías, D. Barchiesi, M. L. De La Chapelle, "Improved analytical fit of gold dispersion: application to the modeling of extinction spectra with a finite-difference time-domain method", Phys Rev B., 71(8): 085416, (2005).
[22] G. M.Jassam, and S. S. Ahmed, "D-shaped photonic crystal fiber toxic metal ions (arsenic) sensor based on surface plasmon resonance", Iraqi Journal of Physics, 21(2), 91-98(2023).

مستشعر الدواء من الألياف البلورية الضوئية يعتمد على رنين البلازمون السطحي

سالي خالد عباس* و سؤدد سلمان احمد

قسم الفيزياء، كلية العلوم، جامعة بغداد، العراق، بغداد

*البريد الالكتروني للباحث: sallyaljanabi@gmail.com

الخلاصة: تقدم هذه الدراسة مستشعرًا يستخدم تقنية الألياف الكريستالية الضوئية (PCF) وتقنية رنين البلازمون السطحي (SPR). تم تطبيق الذهب (Au) كطبقة رقيقة على ألياف كريستالية ضوئية (PCF)، والتي كانت مغلفة سابقًا بمركب ذهبي مستقر كيميائيًا يُظهر خصائص بلازمونية. كان سمك طلاء الذهب 40 نانومتر. تم تقييم مقاييس الأداء، مثل الحساسية (بما في ذلك حساسية الطول الموجي وحساسية السعة) والقرار، عن طريق المحاكاة عبر برنامج COMSOL. تم تطوير المستشعر المقترح باستخدام طريقة العناصر المحدودة ومن ثم إخضاعه للتحليل العددي. تشير النتائج إلى أن سطح الألياف البلورية الضوئية، عند تغليفه بمادة Au، يعمل كجهاز استشعار للكشف عن معامل الانكسار (IR) للعينات الصيدلانية منتهية الصلاحية. يتم إجراء بحث حول تأثيرات المعلمات الهيكلية على أطياف الرنين بهدف تحسين أداء الاستشعار. أعلى حساسية للسعة المسجلة كانت 31.2 RIU-1، في حين أن الحد الأقصى للدقة التي تم الوصول إليها كان 6×10-5 RIU. تم الحصول على هذه القياسات ضمن نطاق الكشف من 1.383 إلى 1.399.